Supplementary Figure Legends

Figure S1. Chromatin-state map of the HOXC locus in breast cancer cells. Histone modification and transcription factor binding across the *HOXC* locus, sourced from publically available ChIP-Seq data (Hg18), see Table S9.

Figure S2. *HOTAIR* alternative promoter produces extra exons 5' to the *HOTAIR* transcript. **(A)** RNA-Seq (GSE30567) analysis of the *HOTAIR* gene showing both positive and negative strands, indicating the start of the *HOTAIR* transcript. Graph Y-axis is indicative of the sequencing reads. Below, HOTAIR transcripts as annotated by RefSeq (73), Broad (74), sequence results for the PCR done in B and the *HOTAIR* promoters are shown as black lines. **(B)** S1 and S2 indicate endpoint PCR results of MCF7 cDNA complimenting RNA-Seq results (A).

Figure S3. Analysis of transcription factor binding and the association of high conservation with each promoter fragment chosen for luciferase reporter assays. From top to bottom are the regions cloned for *HOXC10* (C10)*, HOTAIR* (P1) and *HOXC11* (C11) pGL3 promoter constructs. Predicted transcription factor tracks were sourced from ENCODE data available on the UCSC genome browser (77). Conservation shown is for the vertebrate group within the 46 species analysis on the human genome (Hg19). Histone methylation patterns indicative of active promoters are not shown but were strongly taken into consideration. Promoter primers listed in Table S7.

Figure S4. Putative *HOTAIR* distal enhancer reporter activity demonstrates augmentation of *HOTAIR* promoter across cell lines. (A and C) Schematic of vectors for luciferase assay. Promoters are from Figure S2. **(B and D)** Luciferase reporter activity for pGL3 constructs in MCF7, T47D and MDA-MB-453. Y-axis is relative light units (RLU) based on normalization to Renilla (pRL-TK) transfection control and pGL3-Basic (vehicle). All statistical tests performed were two-tailed *t*-Tests with P-values equal to <0.05 (*), <0.01 (**), <0.001 (***) and <0.0001 (****).

Figure S5. Demonstration of RNA production from alternative HOTAIR promoter in MCF7 cells. RNA-Seq (GSE30567) analysis of the *HOTAIR* gene showing both positive and negative strands, indicating the start of the *HOTAIR* transcript. Graph Y-axis is indicative of the sequencing reads. Below, HOTAIR transcripts as annotated by RefSeq (73) and Broad (74).

Figure S6. FOXA1 knockdown affects expression of HOXC genes in MDA-MB-453 cells. **A and B,** Analysis of HOXC gene expression in MDA-MB-453 breast cancer cells following knockdown of FOXA1 (n=6). Data is normalized to RPLP0 and the scrambled control in A and in B, expression normalized to RNU6B and RPLP0. Statistical significance was tested via two-tailed *t*-Tests with P values equal to <0.05 (*), <0.01 (**), <0.001 (***) and <0.0001 (****).

Figure S7. *HOTAIR* hierarchical clusters display differential hormone receptor status and PAM50 classification. (A) Distribution of tumor hormone receptor (HR) IHC status for clusters 1 and 2. **(B)** Distribution of PAM50 molecular subtype classifications between clusters 1 and 2. Data sourced from TCGA (79).

Figure S8. The combination of *HOTAIR* and *FOXM1* expression stratifies luminal subtypes. The average expression of *HOTAIR* combined with *FOXM1*, across the PAM50 intrinsic subtypes of breast cancer. Data is relative expression, based on RSEM expression quantification from the TCGA dataset (79). Tumor numbers for each subgroup are as follows, Basal-like (140, Basal), HER2-enriched (67, HER2), Luminal A (420, LumA) Luminal B (194, LumB) and Normal-like (24, N-Like).

Figure S9. MCF7 positive control gene expression response to estrogen treatment. (A) Expression for *ERS1*, *PGR*, *MYC* and *FOS* as positive control genes for the appropriate response to estrogen stimulation, done for RNA-Seq. **(B)** Expression for *TFF1* to confirm appropriate response to MCF7 cells responding to estrogen stimulation for the qRT-PCR experiments.

Supplementary Tables

Table S1. Pearson correlation coefficients for Figure 5A Manhattan hierarchical clustering and their corresponding p-values.

Table S2. *HOTAIR* or *FOXM1* alone or in combination significantly stratify the survival of patients with ER+ breast tumors. ER positivity was determined by gene expression in Kaplan-Meier Plotter (78).

Table S3. *HOTAIR* or *FOXM1* alone or in combination significantly stratify the survival of patients with ER+/N+ breast tumors. ER positivity was determined by gene expression in Kaplan-Meier Plotter (78).

Table S4. *HOTAIR* or *FOXM1* alone or in combination significantly predicts response to therapy for patients with ER+ or ER+/N+ breast tumors, through stratification of relapse free survival. Treatment indicated in second column, patients received only tamoxifen (Tam) or only endocrine therapy (ET) or the combination of ET and chemotherapy (CT). ER positivity was determined by gene expression in Kaplan-Meier Plotter (78).

Table S5. *HOTAIR* and its associated transcription factors significantly stratify the relapse free survival of breast cancer patients with tumors based on intrinsic molecular subtypes. Kaplan-Meier survival analysis performed through the online database Kaplan-Meier Plotter (78).

Table S6. Primer sequences for 3C-qPCR analysis of relative interaction frequencies in *Hind*III 3C assays.

Table S7. Primer sequences for *HOXC* promoter constructs for cloning into pGL3 and subsequent luciferase reporter assays.

Table S8. TaqMan® Assay IDs for probes used in qRT-PCR assays.

Table S9. GEO and EBI accession codes for ChIP-Seq, RNA-Seq and ChIA-PET data.

Figure S1. Chromatin-state map of the *HOXC* Locus in breast cancer cells.

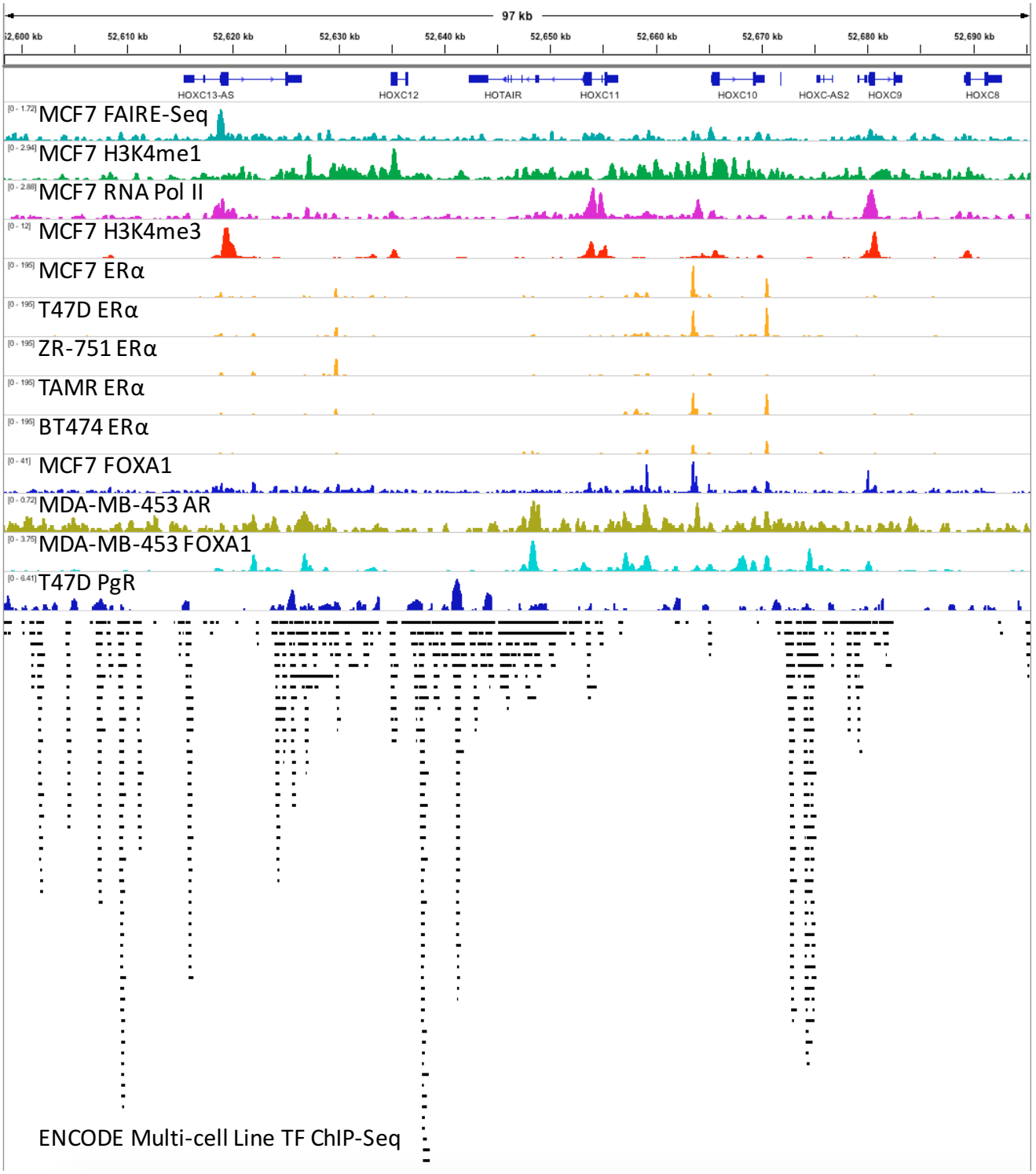

Figure S2. *HOTAIR* alternative promoter produces extra exons 5' to the *HOTAIR* transcript

A

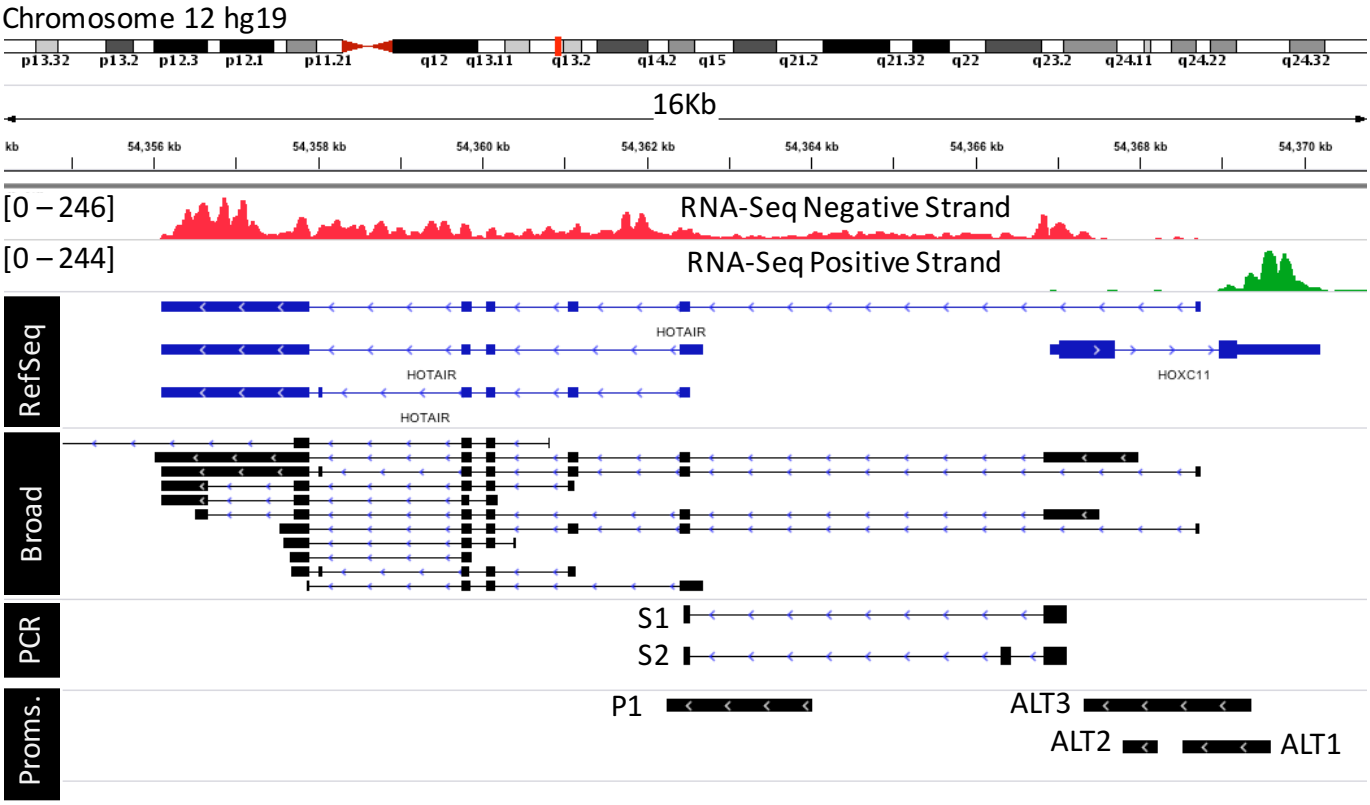

B

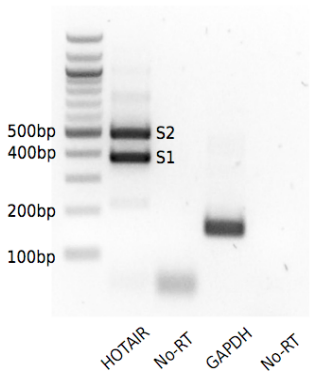

Figure S3. Analysis of transcription factor binding and the association of high conservation with each promoter fragment chosen for luciferase reporter assays

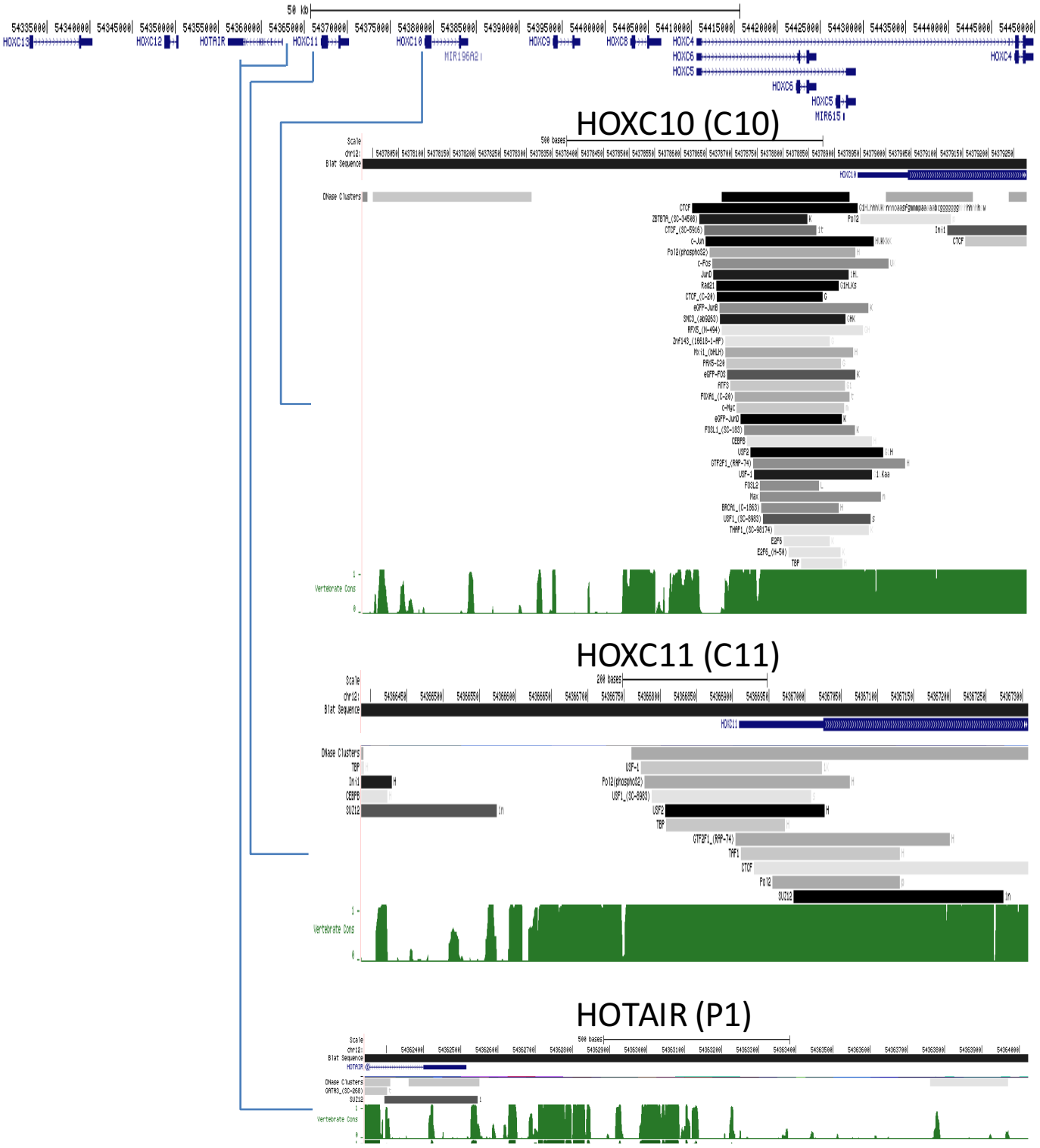

Figure S4. Putative *HOTAIR* distal enhancer reporter activity demonstrates augmentation of *HOTAIR* promoter across cell lines

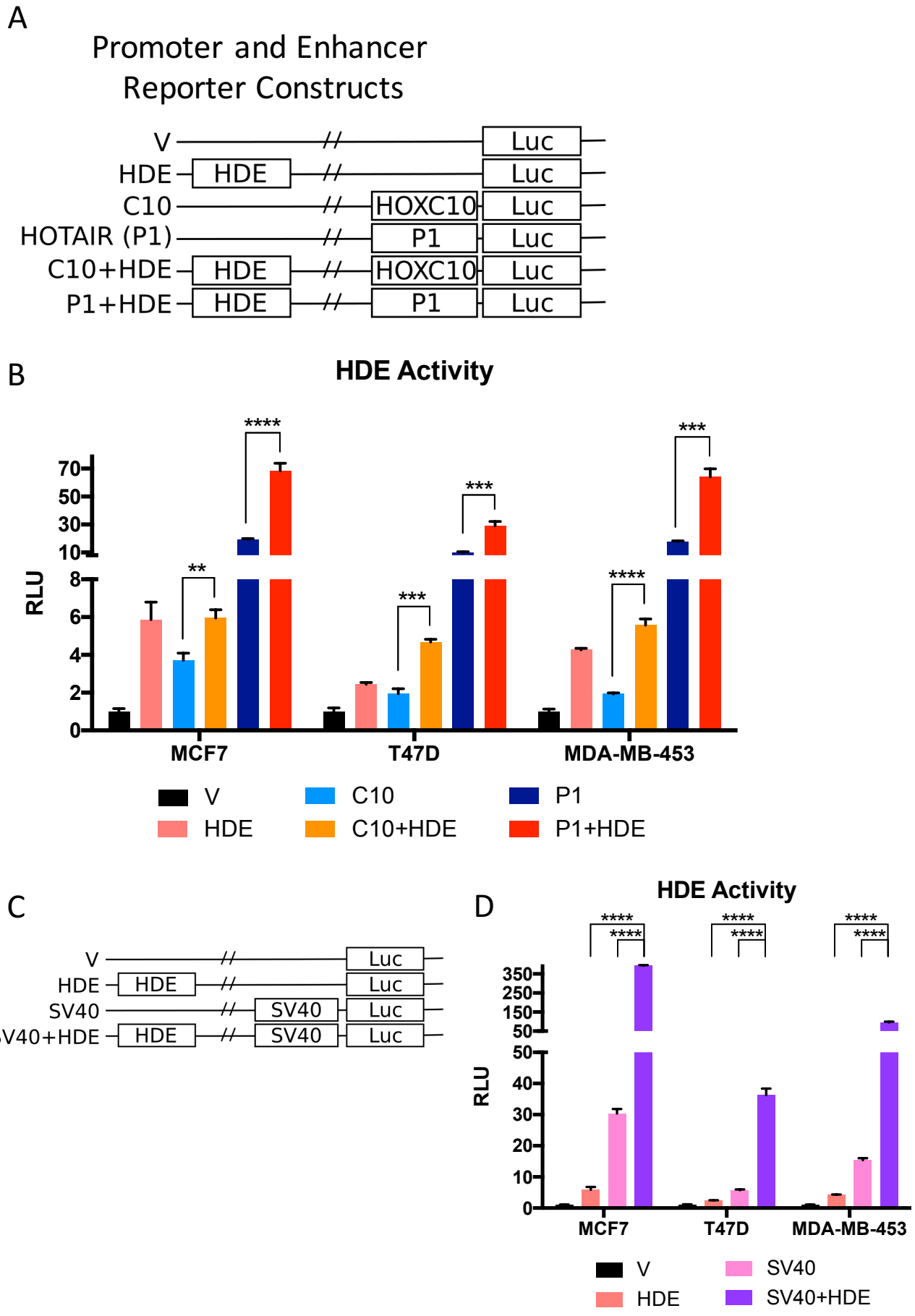

Figure S5. Demonstration of RNA production from alternative HOTAIR promoter in MCF7 cells.

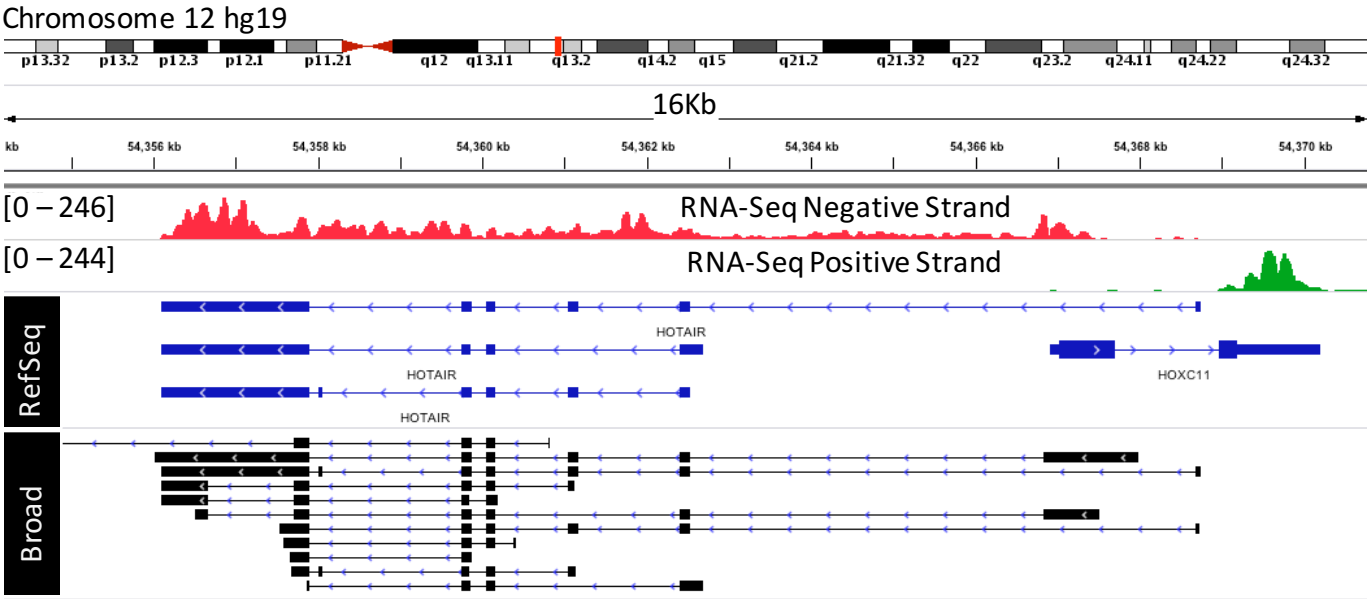

Figure S6. FOXA1 knockdown affects expression *HOXC* genes in MDA-MB-453 cells.

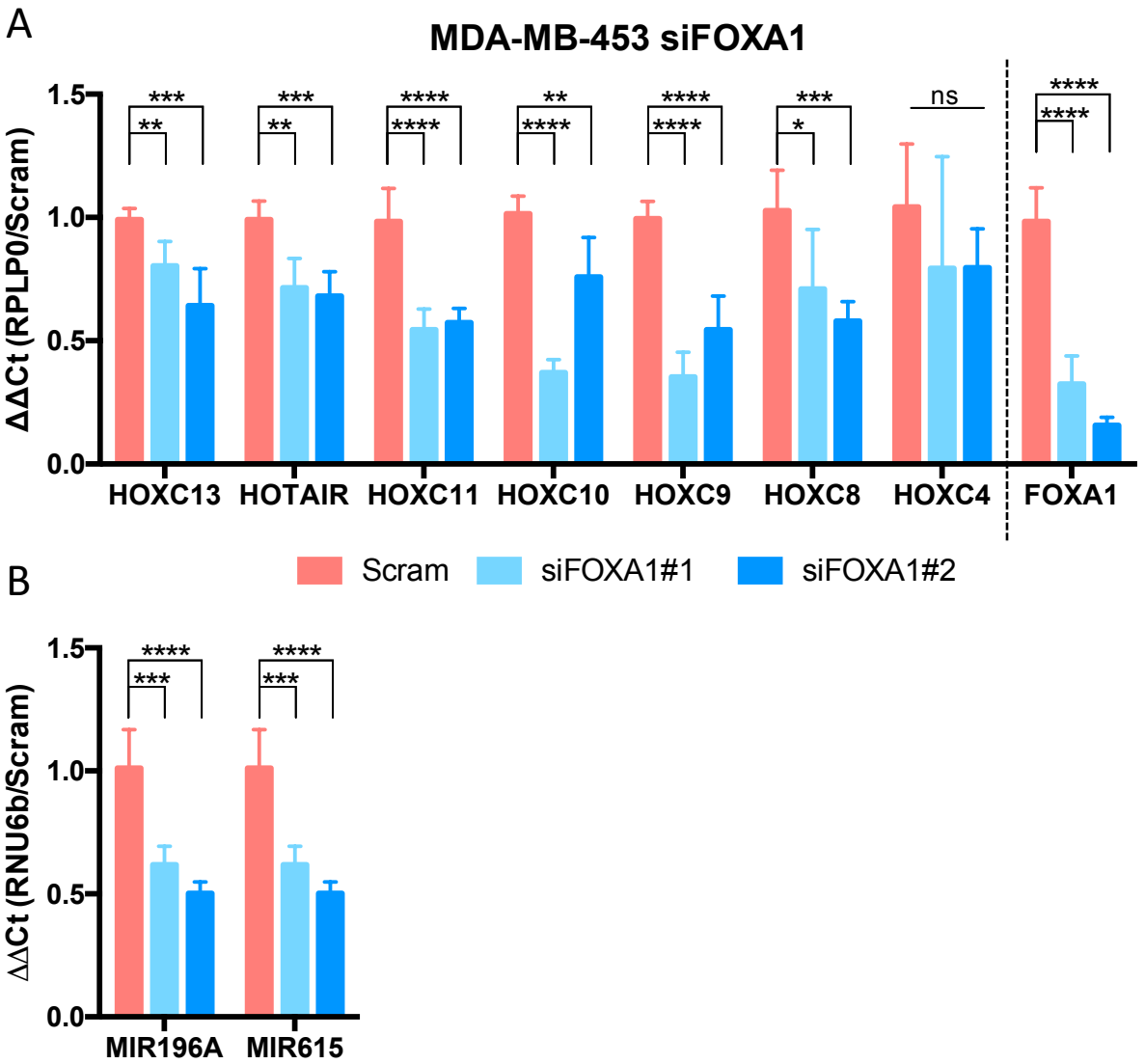

Figure S7. *HOTAIR* hierarchical clusters display differential hormone receptor status and PAM50 classification

A)

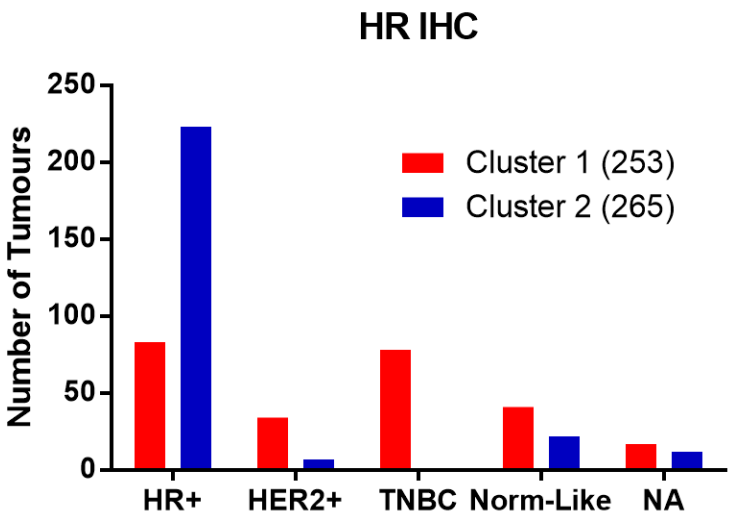

	Cluster 1	Cluster 2
HR+	83	223
HER2+	34	7
TNBC	78	1
Norm-Like	41	22
NA	17	12
	253	265

χ^2 Test P = < 0.0001

B)

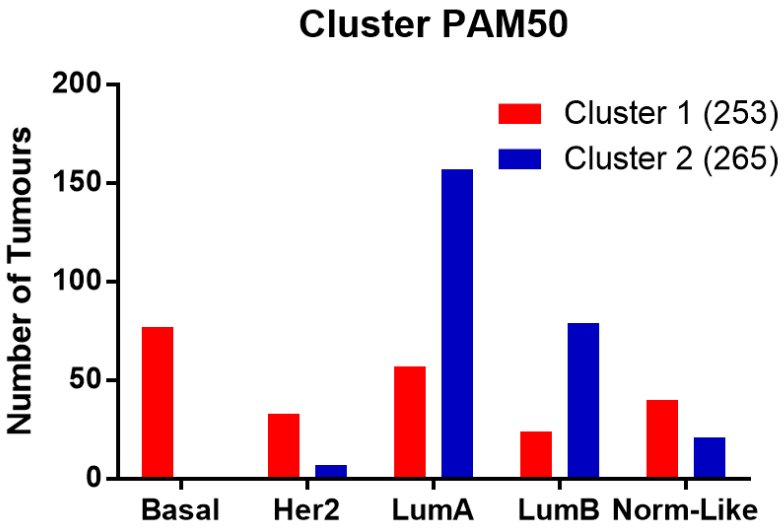

	Cluster 1	Cluster 2
Basal	77	1
Her2	33	7
LumA	57	157
LumB	24	79
Norm-Like	40	21
NA	22	0
	253	265

χ^2 Test P = < 0.0001

Figure S8. The combination of *HOTAIR* and *FOXM1* expression stratifies luminal subtypes

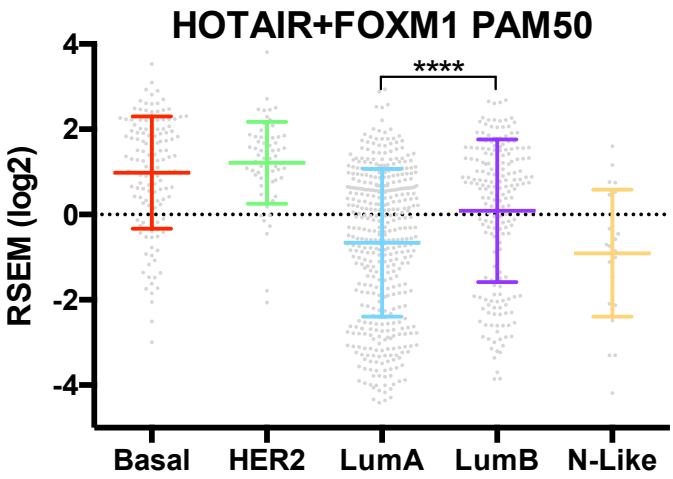

Figure S9. MCF7 positive control gene expression response to estrogen treatment

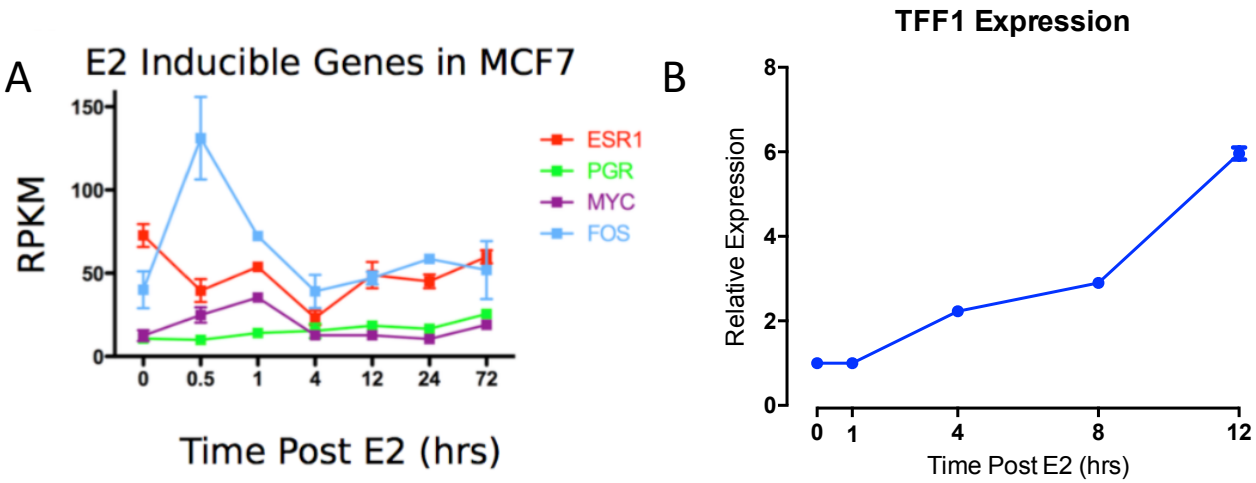

Table S1. Pearson correlation coefficients for Figure 5A Manhattan hierarchical clustering and their corresponding p-values.

NAME	Cluster 1	Cluster 2	Correl All
HOXC12	0.661	0.269	0.524
	1.40E-34	4.41E-06	6.10E-40
HOXC11	0.777	0.463	0.732
	1.23E-54	1.89E-16	5.01E-93
HOXC10	0.793	0.386	0.766
	2.86E-58	1.62E-11	8.22E-107
HOXC13	0.678	0.525	0.725
	6.00E-37	2.04E-21	3.60E-90
HOTAIR	1	1	1
	0	0	0
FOS	-0.210	0.122	-0.030
	5.76E-04	4.01E-02	4.78E-01
FOXM1	0.427	-0.028	0.141
	3.93E-13	6.34E-01	9.08E-04
HOXC9	0.431	0.147	0.499
	2.15E-13	1.31E-02	8.88E-36
HOXC8	0.364	0.279	0.464
	1.13E-09	1.82E-06	1.39E-30
HOXC4	0.045	0.093	0.144
	4.71E-01	1.19E-01	7.49E-04
HOXC5	0.135	0.097	0.299
	2.87E-02	1.05E-01	9.38E-13
HOXC6	0.153	0.072	0.284
	1.31E-02	2.30E-01	1.30E-11
TLE3	-0.524	-0.091	-0.168
	4.99E-20	1.28E-01	8.05E-05
NCOA3	0.217	-0.093	0.154
	3.93E-04	1.18E-01	2.97E-04
JUN	0.087	0.084	0.082
	1.57E-01	1.57E-01	5.56E-02
GREB1	-0.603	0.049	-0.059
	1.59E-27	4.08E-01	1.66E-01
FOXA1	-0.386	0.109	0.000
	8.47E-11	6.68E-02	9.93E-01
GATA3	-0.544	0.022	-0.092
	9.67E-22	7.12E-01	3.11E-02
ESR1	-0.692	0.007	-0.177
	6.14E-39	9.09E-01	3.24E-05
Tumour #	264	279	543
Tumour %	48.62%	51.38%	

Table S2. *HOTAIR* or *FOXM1* alone or in combination significantly stratify the survival of patients with ER+ breast tumors. ER positivity was determined by gene expression in Kaplan-Meier Plotter.

	Gene	Survival	Logrank			Tumour #	
			HR	95% CI	P-Value	Low	High
ER+ (Gene Expression)	HOTAIR	RFS	1.43	(1.15 - 1.77)	1.20E-03	368	637
		DMFS	2.51	(1.49 - 4.22)	3.20E-04	123	221
		OS	1.63	(1.01 - 2.64)	4.40E-02	163	71
		PPS	1.68	(1.00 - 2.82)	4.80E-02	58	28
	FOXM1	RFS	2.31	(1.90 - 2.80)	1.00E-16	544	1636
		DMFS	2.58	(2.02 - 3.29)	1.80E-15	647	292
		OS	3.71	(2.55 - 5.39)	2.30E-13	202	305
		PPS	1.83	(1.25 - 2.68)	1.70E-03	67	178
	FOXM1 + HOTAIR	RFS	2.31	(1.74 - 3.08)	3.00E-09	251	754
		DMFS	2.06	(1.35 - 3.14)	6.70E-04	242	102
		OS	2.03	(1.26 - 3.27)	3.00E-03	166	68
		PPS	1.73	(1.02 - 2.94)	4.10E-02	34	52

Table S3. *HOTAIR* or *FOXM1* alone or in combination significantly stratify the survival of patients with ER+/N+ breast tumors. ER positivity was determined by gene expression in Kaplan-Meier Plotter.

	Gene	Survival	Logrank			Tumour #	
			HR	95% CI	P-Value	Low	High
ER+/N+ (Gene Expression)	HOTAIR	RFS	1.58	(1.09 - 2.28)	1.40E-02	166	283
		DMFS	1.87	(0.70 - 4.97)	2.00E-01	35	52
	FOXM1	RFS	2.65	(1.91 - 3.65)	5.80E-10	224	405
		DMFS	2.49	(1.41 - 4.41)	1.20E-03	90	126
	FOXM1 + HOTAIR	RFS	3.23	(1.89 - 5.53)	6.20E-06	112	337
		DMFS	6.64	(0.89 - 49.8)	3.30E-02	22	65

Table S4. *HOTAIR* or *FOXM1* alone or in combination significantly predicts response to therapy for patients with ER+ or ER+/N+ breast tumors, through stratification of relapse free survival. Treatment indicated in second column, patients received only tamoxifen (Tam) or only endocrine therapy (ET) or the combination of ET and chemotherapy (CT). ER positivity was determined by gene expression in Kaplan-Meier Plotter.

	Gene	Treat.	Logrank			Tumour #	
			HR	95% CI	P-Value	Low	High
ER+ (Gene Expression)	HOTAIR	Tam	1.74	(0.66 - 4.58)	2.50E-01	65	26
		ET	1.58	(0.84 - 2.98)	1.50E-01	87	71
		ET/CT	2.11	(1.02 - 4.38)	4.10E-02	96	40
	FOXM1	Tam	2.88	(2.12 - 3.91)	1.50E-12	359	182
		ET	2.74	(2.08 - 3.60)	7.30E-14	438	232
		ET/CT	4.22	(1.96 - 9.11)	6.70E-05	86	50
	FOXM1 + HOTAIR	Tam	8.43	(1.93 - 36.9)	6.90E-04	47	44
		ET	3.69	(1.70 - 8.05)	4.20E-04	75	83
		ET/CT	3.41	(1.54 - 7.05)	4.80E-04	101	35
ER+/N+ (Gene Expression)	HOTAIR	Tam	0.59	(0.19 - 1.82)	3.50E-01	11	32
		ET	0.58	(0.22 - 1.53)	2.60E-01	16	37
		ET/CT	1.78	(0.79 - 4.01)	1.60E-01	84	29
	FOXM1	Tam	2.96	(1.52 - 5.76)	8.50E-04	43	118
		ET	2.74	(1.48 - 5.07)	8.10E-04	51	121
		ET/CT	5.84	(2.31 - 14.7)	2.30E-05	69	44
	FOXM1 + HOTAIR	Tam	4,24	(0.94 - 19.2)	4.10E-02	18	25
		ET	3.51	(1.03 - 12.0)	4.40E-02	12	41
		ET/CT	3.38	(1.54 - 7.42)	1.30E-03	84	29

Table S5. *HOTAIR* and its associated transcription factors significantly stratify the overall survival of breast cancer patients with tumors based on intrinsic molecular subtypes. Kaplan-Meier survival analysis performed through the online database Kaplan-Meier Plotter.

	Subtype	Logrank			Tumour #	
		HR	95% CI	P-Value	Low	High
HOTAIR	Basal	1.96	(0.68 - 5.69)	2.00E-01	33	87
	LumA	1.38	(0.70 - 2.73)	3.50E-01	46	103
	LumB	2.54	(1.17 - 5.51)	1.40E-02	54	31
	HER2	4.36	(1.66 - 11.5)	1.10E-03	36	20
	ER+ (GE)	1.63	(1.01 - 2.64)	4.40E-02	163	71
TFs	Basal	0.62	(0.34 - 1.12)	1.10E-01	43	126
	LumA	0.66	(0.43 - 1.01)	5.30E-02	81	194
	LumB	1.22	(0.73 - 2.06)	4.50E-01	57	175
	HER2	1.95	(0.91 - 4.20)	8.30E-02	41	26
	ER+ (GE)	0.83	(0.58 - 1.18)	3.00E-01	378	129
HOTAIR + TFs	Basal	0.48	(0.21 - 1.09)	7.30E-02	31	89
	LumA	2.49	(1.05 - 5.89)	3.20E-02	37	112
	LumB	1.73	(0.65 - 4.60)	2.60E-01	23	62
	HER2	6.03	(1.39 - 26.2)	6.40E-03	24	32
	ER+ (GE)	1.47	(0.92 - 2.36)	1.10E-01	146	88

Table S6. Primer sequences for 3C-qPCR analysis of relative interaction frequencies in *Hind*III 3C assays.

Oligo Name	Sequence (5' to 3')	Application
HOXC_ENH1_DW3F	GGATGAGATGGGAGGAGTGGGGTAGG	HindIII Fragment 1
HOXC_ENH1_dw2R	AGGCAATCGATCAGAGTCGCCCTGG	HindIII Fragment 2
HOXC_ENH1_dw1R	GACCAATCCACTACAGGCCAAATGTACACC	HindIII Fragment 3
HOXC_ENH1_IntR	GGTCAGTCTGAGAAACCTTCGTGGAAGAGG	HindIII Fragment 4
HOXC_ENH1_up1R	CCAGATGCTACCAGCACACACCGTTAGG	HindIII Fragment 5
HOXC_ENH1_up2F	CCTGCCCTCACCACACACAAGTGTG	HindIII Fragment 6
HOXC_ENH1_up3R	CCTGGATGCCTCAGCAAGGATTGTCAG	HindIII Fragment 7
HOXC_ENH1_up4R	GGAAGTTTGGCCTCATGGCTCCTGC	HindIII Fragment 8
HOXC_ENH1_up5R	CCTCAGGGCCTTTGTACTTGCTGTCCAC	HindIII Fragment 9
HOXC_ENH1_up6F	GGTCTACCTGCTCAGAGAGTACACAGCTGAGG	HindIII Fragment 10
HOXC_ENH1_up7R	GGTTTAAGCGAAGAGCTGGCAGGATGC	HindIII Fragment 11
HOXC_ENH1_up8R	CCATCCCCTTCAATCCTCCCTTTAACTCC	HindIII Fragment 12
HOXC_ENH1_up9F	AAGGAAGCACAATGGGCACCCTGTCC	HindIII Fragment 13
HOXC_ENH1_up10F	GCTGTCTTTTCCCTGGAATTCCTTCCTCC	HindIII Fragment 14
HOXC_ENH1_up11F	CTCACCCCTGTCTCCAATCCTCTTAACTCC	HindIII Fragment 15
HOXC_ENH1_up12R	CCTTAGGCCACCCATGTCAATGTCTAGC	HindIII Fragment 16
HOXC_ENH1_up13R	CCAAGCCGCCTGCTTATTCCAACC	HindIII Fragment 17
HOXC_ENH1_up14R	ATGTGCCTTCCCACCTCCATTATTGAGG	HindIII Fragment 18
HOXC_ENH1_up15R	GCTTGTGTAGGCCCACAGGAATACACC	HindIII Fragment 19
HOXC_ENH2_Int2R	CCGTCTTACCACACCCTCC	HindIII Fragment 20
HOXC_ENH3_Int3R	CTCAGGGAATGTGAGTCAATCCAACTCG	HindIII Fragment 21
HOXC_ENH3_up1R	GGATGACACTATCTCACAGCCAAAGACACC	HindIII Fragment 22
HOXC_ENH3_up2R	GACTGGCTGACACCATGATGCTTTTGC	HindIII Fragment 23
HOXC_ENH3_up3R	CTCCCAAACATCGAACCCCCTAAAATGG	HindIII Fragment 24
HOXC_ENH3_up4R	CAGGCTGATCTCCCCTGTAATCCATGC	HindIII Fragment 25
HOXC_ENH4_Int4F	TCCCTCTTTGACACTCAGTTTTGTGACTCTGG	HindIII Fragment 26
HOXC_ENH5_Int5R	CTCTTCCAAGCAGCCTTCTCAGATCTTTCC	HindIII Fragment 27
HOXC_ENH5_up1R	CTCTGTGCTGCAAACTCCTAGTGTTCCTCC	HindIII Fragment 28
HOXC_ENH5_up2F	CCTGGGTGGAGGAGTGAGAAGACATACC	HindIII Fragment 29
HOXC_ENH6_Int6R	GAGCTCTGCTGCTTGCAGTGGAATGG	HindIII Fragment 30
HOXC_ENH7_Int7R	CCATGAGAGGGCACAGGGCAGAATG	HindIII Fragment 31
HOXC_ENH7_up1R	GAAGAAAGCAAAAGCCCCTACCTCACAGG	HindIII Fragment 32
HOXC_ENH7_up2F	GGAGTATTGGTAGGTGTGGGAGGCAGG	HindIII Fragment 33
HOXC_ENH7_up3R	TGCTTCCTCCACCATGCTTATGCTGG	HindIII Fragment 34
HOXC_ENH7_up4R	CTGCCCGTTGACCATTCTAAGCAACC	HindIII Fragment 35
HOXC_ENH8_Int8F	GAGGTTGCAGTGAGCCAAGATTGTGC	HindIII Fragment 36
HOXC_ENH8_up1F	CTCTTCCATTAATTGGCAGAGGCAGAATGG	HindIII Fragment 37
HOXC_ENH8_up2F	GCATCCTGCAACAGAGGGATTTGTTCC	HindIII Fragment 38
HOXC13_Dw3F	GCAGATGATTCTTGCCAGTGGGTGG	HindIII Fragment 39
HOXC13_Dw2F	CCACTGTGTGAGGCGGGTTTACAGC	HindIII Fragment 40
HOXC13_Dw1R	CAGAAGACCCATTTCACCATCTTGGAGC	HindIII Fragment 41
HOXC13_geneR	CAGTGCTTGGCTTATTAATGAATTTCCCTCC	HindIII Fragment 42
HOXC13b_Int8R	CACACTAAACCCATTGCACATTGCTCTGG	HindIII Fragment 43
HOXC12_geneR	CAAAAGGAGGTGCCTAGCTCCACATGG	HindIII Fragment 44
HOTAIRa_geneR	GATGGCAGCACACCTATGAACAGACATTCG	HindIII Fragment 45
HOTAIRb_geneF	CAGGCGATAAATCTCTGGCGAATCTTCC	HindIII Fragment 46
HOXC11_Int9R	CTGCCTTCTGCCTGCACATTCTGC	HindIII Fragment 47
HOXC10prom_Int10aF	TTCGGAACCTCCTTTTCCGAGCAGC	HindIII Fragment 48
HOXC10_Int10b_Int11aR	GGACCCGACTCCCACTTCTTACCTTGG	HindIII Fragment 49
MIR196b_Int11bR	GTGCTCTGGAGCCACTTCCAATCAGG	HindIII Fragment 50
HOXC9_geneR	CTGAGAACAGGGGTGTATCTCCTCAGTCTCC	HindIII Fragment 51

HOXC8_geneR	CCTGCTATGGGTAGAGGAGAGGGTCAGAGG	HindIII Fragment 52
HOXC8_up1R	GACAGTGATGACAATCTTCCTGTGCAGAGG	HindIII Fragment 53
HOXC8_up2R	TGCGATGCATTTGTGTAGCGTGTGC	HindIII Fragment 54
HOXC8_up3F	GCATTGGAGAGGACTGGAGAAGCAAGTG	HindIII Fragment 55
HOXC6_HOXC5_Int12F	GTTCCACCTGGAAACAGGGCAAACG	HindIII Fragment 56
HOXC5_up1R	GGATGGGAAGAGCGAGACAGAGACCCA	HindIII Fragment 57
HOXC5_up2R	TGAGGGTGGACTAGAGACTTCGCAAGTGC	HindIII Fragment 58
HOXC4a_geneR	GTTAGTTAGAGGTTGGGTTCCCCACCACC	HindIII Fragment 59
HOXC4b_geneR	GTTAGTTAGAGGTTGGGTTCCCCACCACC	HindIII Fragment 60

Oligo Name	**Sequence (5' to 3')**	**Application**
GAPDH_F	TGATGACATCAAGAAGGTGGTGAAGCAGG	3C Neg. Ctrl
GAPDH_R	CCTCAACGACCACTTTGTCAAGCTCATTTC	3C Neg. Ctrl
HindIII_Dig_EffF	TTGTTGCTGTCCTCTAGGCAGC	3C Dig. Effic (+ve ctrl)
HindIII_Dig_EffR	CCTGTTAACACCCCTCCCTAACA	3C Dig. Effic (+ve ctrl)

Table S7. Primer sequences for HOXC promoter constructs for cloning into pGL3 and subsequent luciferase reporter assays.

Oligo Name	Seq 5' to 3'
HDE_FOW	GGCTAATTTTGTATTTTTAGTAGAGACG
HDE_REV	CTGGAAAAGGGTACTTCAAACC
HOT_Prom_F	CCTATCTGGTGGGTGCCTGT
HOT_Prom_R	TCTCTGGCGAATCTTCCTGT
HC10_Prom_F	CAGGGCCTGAAGTAAAGCAG
HC10_Prom_R	AGTCCAGCTGCGAGAGGTAG
HC11_Prom_F	CTCTGGCCAGGAAAAGAGTGG
HC11_Prom_R	CCGCATAGCAGGAGGAGTAGC
ALT1_Prom_F	CTCTCGCCAGATTTCACTGC
ALT1_Prom_R	TTAGCGGATCTTTTCACATGG
ALT2_Prom_F	CTCGTGTTTTGGGTCAGTCC
ALT2_Prom_R	GTCCTGGCTTGCCTCTCC
ALT3_Prom_F	GAGTGCCTGCCTCCTTCC
ALT3_Prom_R	TAGAGGGTCCAGGAGGTTC

Table S8. Taqman Assay IDs for probes used in qRT-PCR assays.

Gene Name	Taqman Assay ID
ESR1	Hs00174860_m1
FOXA1	Hs04187555_m1
FOXM1	Hs01073586_m1
HER2	Hs01001580_m1
HOTAIR Probe1 (HOTAIR)	Hs03296680_s1
HOTAIR Probe2	Hs03296631_m1
RPLP0	Hs99999902_m1

Table S9. GEO and EBI accession codes for ChIP-Seq, RNA-Seq and ChIA-PET data.

Experiment	GEO
MCF7 Histone	GSE23701
Breast Cell Line ER, FoxA1	E-MTAB-223
MDA-MB-453 AR and FoxA1	E-MTAB-986
T47D PGR	GSE30871
Breast tumour ER	GSE32222
RNA-Seq MCF7	GSE30567
ChIA-PET ER, RNA Pol II and CTCF	GSE39495
GRO-Seq ER	GSE27463
MCF7 cFos	GSE26831
MCF7 FoxM1	GSE40767
MCF7 E2F1	GSE28286